Electronic Transport in Phosphorus-Doped Silicon Nanocrystal Networks

A. R. Stegner, R. N. Pereira,* K. Klein, R. Lechner, R. Dietmueller, M. S. Brandt, and M. Stutzmann
Walter Schottky Institut, Technische Universität München, Am Coulombwall 3, 85748 Garching, Germany

H. Wiggers
Institut für Verbrennung und Gasdynamik, Universität Duisburg-Essen, 47048 Duisburg, Germany
(Received 25 July 2007; published 16 January 2008)

We have investigated the role of doping and paramagnetic states on the electronic transport of networks assembled from freestanding Si nanocrystals (Si-NCs). Electrically detected magnetic resonance (EDMR) studies on Si-NCs films, which show a strong increase of conductivity with doping of individual Si-NCs, reveal that P donors and Si dangling bonds contribute to dark conductivity via spin-dependent hopping, whereas in photoconductivity, these states act as spin-dependent recombination centers of photogenerated electrons and holes. Comparison between EDMR and conventional electron paramagnetic resonance shows that different subsets of P-doped nanocrystals contribute to the different transport processes.

DOI: 10.1103/PhysRevLett.100.026803 PACS numbers: 73.50.−h, 61.46.Hk, 68.55.Ln, 76.30.−v

Doping of semiconductor nanocrystals has proven to be quite distinct from the corresponding bulk materials [1–4]. This has been attributed to effects such as self-purification and the increase of the donor ionization energy, leading to a reduced electron concentration at room temperature [5,6], as well as to the dependence of dopant adsorption on surface morphology and nanocrystal shape during growth [7]. The future exploitation of semiconductor nanocrystals depends on the understanding and control of their electronic doping, and also on their electronic transport properties. However, the effect of dopants on the electronic transport of semiconductor nanocrystals has not yet been investigated, due to difficulties in the preparation of samples that can be used in such studies. In the case of Si nanocrystals (Si-NCs), previous investigations of doping have only dealt with nanocrystals embedded in glass matrices, which are formed upon thermal annealing of amorphous films fabricated by co-sputtering of Si and phosphosilicate glass [8,9]. In this case, the insulating nature of the oxide matrix impedes the use of such samples for the investigation of electronic transport in doped Si-NCs. In this work, we circumvent this problem by investigating thin films of densely packed Si-NCs, which are formed from macroscopic quantities of isolated P-doped Si-NCs with selected diameters. Using electron paramagnetic resonance (EPR), we establish the incorporation of substitutional P atoms in the Si-NCs. The effect of doping on the electrical transport of Si-NCs is studied by temperature dependent conductivity measurements. Furthermore, we have investigated the influence of dopants and defects on spin-dependent transport using electrically detected magnetic resonance (EDMR), where spin-dependent electronic transport involving paramagnetic states is detected via resonant current changes. Hence, paramagnetic states taking part in electronic transport can be directly identified. Spin-dependent electronic transport involving P donors and Si dangling bonds (Si-DBs) has recently been shown to be a promising mechanism for the electrical readout of coherent ^{31}P spin states [10], which is a fundamental requirement in spin-based quantum computation schemes [11,12]. Here, we demonstrate that P states and Si-DBs participate in spin-dependent electronic transport also in P-doped Si-NCs, suggesting that spin-to-charge transfer mechanisms could also be achieved in Si-NCs. Distinct spin-dependent transport mechanisms are observed in dark and photoconductivity.

Freestanding Si-NCs in powder form were produced by microwave-induced decomposition of silane in a low-pressure microwave plasma reactor. This method yields macroscopic amounts of spherical crystalline Si nanoparticles, with a surface suboxide layer formed after exposure to air [13]. Samples with a mean particle diameter between 4 and 50 nm, as measured by the Brunauer-Emmet-Teller (BET) method [14], were studied. The Si-NCs have a log-normal size distribution with a standard deviation of the diameter of typically $\sigma = 1.5$ [13]. In the present work, P doping was achieved by adding phosphine to the precursor gas. Hereafter, the nominal P doping level is defined as the atomic density of bulk Si multiplied by the fraction of phosphine in the total flow of precursor gases during synthesis. It should be noted that the concentration of P atoms in the Si-NCs is not necessarily the same as the nominal doping concentration, since the incorporation probability of P and Si atoms in the Si-NCs may be different, as discussed for microcrystalline Si [15]. EPR studies were performed in a conventional continuous-wave *X*-band spectrometer using a lock-in amplifier and a TM_{110} cavity. A helium flow cryostat was used for measurements at low temperatures. In EPR studies, the Si-NCs powder (~1.5 mg) was inserted into a small teflon tube inside a suprasil quartz sample holder tube.

Figure 1(a) shows the dependence of the EPR spectra on the doping level for samples of Si-NCs with a mean particle diameter of 46 ± 1 nm. The spectrum of undoped Si-NCs displays only a broad resonance centered at $g \simeq 2.006$, which originates from different configurations of Si-

 © 2008 The American Physical Society

DBs, namely, trivalent Si atoms at the Si/SiO_2 interface (P_b centers) and Si-DBs in a disordered environment [16]. For the Si-NCs doped with $[P] = 1.3 \times 10^{18}$ cm^{-3}, additional features are observed: (i) a line centered at $g = 1.998$ and (ii) two lines, denoted [hf(^{31}P)], located symmetrically at the high and low field side of the $g = 1.998$ line, with a magnetic field splitting of ~4.1 mT. The latter pair of lines is the typical hyperfine signature of substitutional P in crystalline Si (*c*-Si), where the Zeeman states of the donor electron are split by interaction with the ^{31}P nucleus ($I = 1/2$) [17]. The $g = 1.998$ signal in our Si-NCs originates from exchange-coupled substitutional P atoms. A line at $g = 1.998$ is also observed in *c*-Si for intermediate and high P concentrations, and corresponds to clusters of two or more closely spaced P donors [17]. Hence, the observed P-related EPR lines provide clear evidence for the incorporation of substitutional P atoms into the crystalline core of the Si-NCs. In the spectrum of the Si-NCs with $[P] = 1.2 \times 10^{19}$ cm^{-3}, the hf(^{31}P) lines disappear, while the line at $g = 1.998$ increases in intensity, similar to what is observed in heavily P-doped *c*-Si [17,18].

EPR spectra recorded for samples of Si-NCs with mean particle diameters of 4.3 and 11 nm and $[P] = 5 \times 10^{20}$ cm^{-3} are shown in Fig. 1(b). In addition to the signal due to Si-DBs at $g \sim 2.006$, the line at $g = 1.998$ is also observed, which lends experimental evidence for the successful doping of Si-NCs also in the diameter range down to ~4 nm. In Fig. 1(b), the $g = 1.998$ signal is approximately 3 times weaker for the 4.3 nm sample than for the 11 nm sample. Although the nominal doping concentration is the same in the two samples, the effective doping level decreases with decreasing size of the Si-NCs. This can be attributed to different causes, such as a size-dependent incorporation probability of P atoms into Si-NCs (self-purification) or a reduced EPR visibility of P for smaller Si-NCs due to broadening caused by quantum-confinement of the donor electron wave function [5]. Moreover, electron capture by surface Si-DBs, which leads to compensation of donors [19], can be enhanced for smaller Si-NCs, where the surface-to-volume ratio is larger.

Understanding the effect of doping on the electronic transport of networks of Si-NCs is fundamental for any future application. While our EPR data prove that donor electrons are present in P-doped Si-NCs at low temperatures, whether these have a relevant influence on the charge transport properties of Si-NC networks is not clear at this point, since effects such as charge trapping in surface defects, percolation of charge carriers, and nanocrystal ionization at room temperature may obscure any role of doping of the individual nanocrystals. We have studied the electronic transport of Si-NC networks using films composed of undoped and P-doped Si-NCs. For this purpose, Si-NCs were dispersed in ethanol using a ball milling process [20] and spin coated onto flexible Kapton polyimide substrates, with interdigit gold contacts. The gold grids consisted of 112 digits of 10 μm width and 10 μm

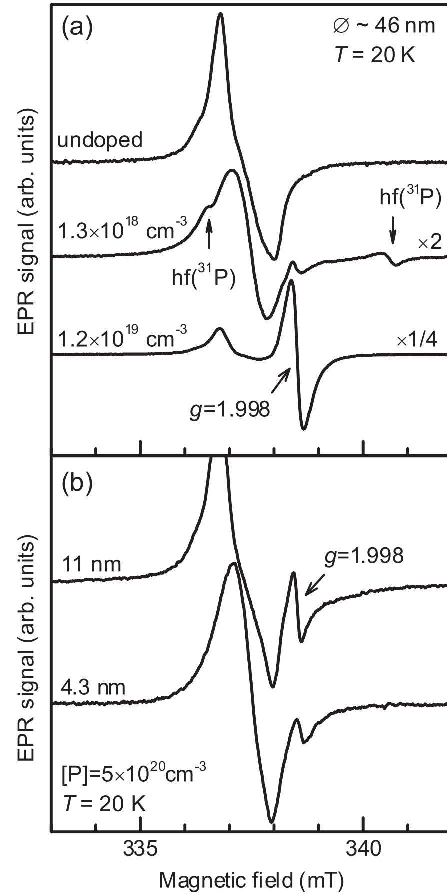

FIG. 1. (a) EPR spectra of undoped Si-NCs and Si-NCs doped with the indicated P concentrations. (b) EPR spectra of doped Si-NCs with mean particle diameters of 11 and 4.3 nm. All spectra were measured under the same experimental conditions, and their intensity was normalized to the sample mass.

spacing. After drying, uniform ~500 nm thick films of densely packed Si-NCs are formed. We find that these are electrically conductive only after etching in dilute hydrofluoric acid (5% in H_2O) for 15 seconds and subsequent washing in deionized water. Before this treatment, the film conductivity is below 10^{-14} Ω^{-1} cm^{-1}. The effect of hydrofluoric acid (HF) etching was probed by infrared absorption spectroscopy carried out with a Fourier-transform spectrometer (see Fig. 2). Before HF etching [curve (i)], the infrared spectrum is dominated by a band located at ~1100 cm^{-1} that originates from O stretching of Si-O-Si bonds at the surface of the Si-NCs [13,21]. In addition, Si-H stretching and wagging modes at 2254 and 880 cm^{-1}, respectively, due to O_3-Si-H units [22,23], and a band at 2115 cm^{-1} from H stretching in Si_{4-x}-Si-H_x ($x = 1, 2, 3$) bonds are also observed [23]. The vibrational modes of oxygen-containing species are removed from the spectrum after HF etching [curve (ii)] and the band at ~2115 cm^{-1} increases in intensity and becomes structured, with peaks at 2086 and 2138 cm^{-1} from the out-of-phase and in-phase stretching of the H atoms of Si_2-Si-H_2 and a peak at 2105 cm^{-1} from the H stretching

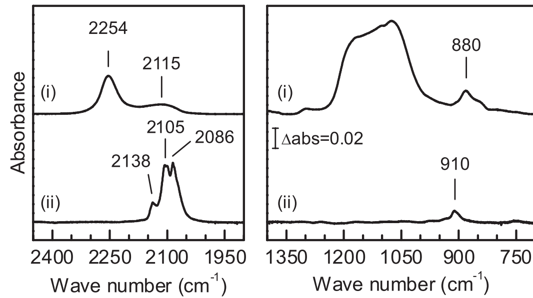

FIG. 2. Infrared absorbance spectra of a film of Si-NCs (∅ ~ 11 nm) measured (i) before and (ii) after HF etching.

in Si_3-Si-H [23]. A weak line from the H scissors mode of Si_2-Si-H_2 is also observed at 910 cm^{-1} [23]. Hence, the etching leads to a removal of the high potential barriers at the surface oxide layer of the Si-NCs, which strongly suppress the tunneling of charge carriers between Si-NCs, and a predominant H termination of Si-NCs over the total volume of the films is attained.

Figure 3 shows the temperature dependence of the conductivity for Si-NCs (30 ± 2 nm) with different doping levels. As can be seen, doping of the Si-NCs strongly influences the electronic transport properties of the films. For the undoped Si-NCs, a thermally activated transport with an activation energy $E_a \sim 0.5$ eV is observed. An increase of the Si-NCs doping concentration results in an increase of the films conductivity and in a decrease of the conductivity temperature dependence.

To investigate the role of paramagnetic states for electronic transport in Si-NCs, we have performed EDMR measurements. Unlike in conventional EPR, in EDMR, only paramagnetic states that are involved in electrical transport are detected via resonant changes of the current through the sample. Spectra were recorded with a constant applied bias field of 10^5 V cm^{-1}, resulting in 0.01–1 μA currents, and magnetic field modulation amplitude and frequency of 0.12 mT and 2 kHz, respectively. EPR and EDMR spectra of a film of Si-NCs (∅ ~ 30 nm) doped with [P] = 1.5×10^{20} cm^{-3} are compared in Fig. 4. The

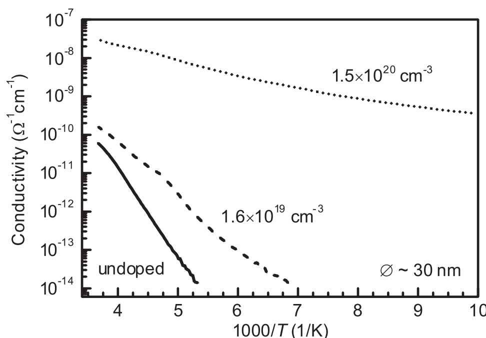

FIG. 3. Arrhenius plot of dark conductivity vs temperature for films of Si-NCs (∅ ~ 30 nm) doped at different levels measured with an applied voltage of 20 V and after HF etching.

EPR spectrum recorded in the dark [curve (a)] shows a signal at $g = 2.0055$ due to Si-DBs [16], and a weaker line at $g = 1.998$ from exchange-coupled donor electrons. No hyperfine doublet from isolated P donors is observed in this EPR spectrum, which is a result of the high doping of the Si-NCs [17], similar to the situation in the EPR spectra of samples with [P] > 10^{19} cm^{-3} shown in Fig. 1. In the dark EDMR spectrum [curve (b)], the $g = 1.998$ line does not appear, but instead, a 1 mT broad band at 340.4 mT, denoted hf(^{31}P), is observed. This line corresponds to the high field hyperfine resonance of isolated P, which has also been observed in the EPR spectrum of Fig. 1(a) for the [P] = 1.3×10^{18} cm^{-3} sample. The low field partner line of the hf(^{31}P) resonance expected at about 336.2 mT is not observed due to overlap with the stronger band at $g = 2.0055$.

The EDMR spectrum in curve (b) establishes that Si-DBs and isolated P states participate in electronic transport in Si-NCs. We have observed that the EDMR resonances in the dark lead to a current enhancement with a maximum relative current change $\Delta I/I = +5 \times 10^{-4}$. In EDMR, transitions between singly occupied electronic states that are spin forbidden due to the Pauli principle become allowed via spin flips in one of the states. Thus, for spin-dependent hopping transitions between singly occupied states, the spin flip leads to an enhancement of the current [24,25], as observed for the dark EDMR spectrum of our film. EDMR measurements carried out under illumination reveal distinct spin-dependent transport mechanisms. Curve (c) in Fig. 4 shows the EDMR spectrum recorded with the same sample, but under white light excitation, which increases the conductivity by a factor of 10. Now, the $g = 1.998$ line is also observed, and the contribution of the P_b surface centers to the dangling bond-related reso-

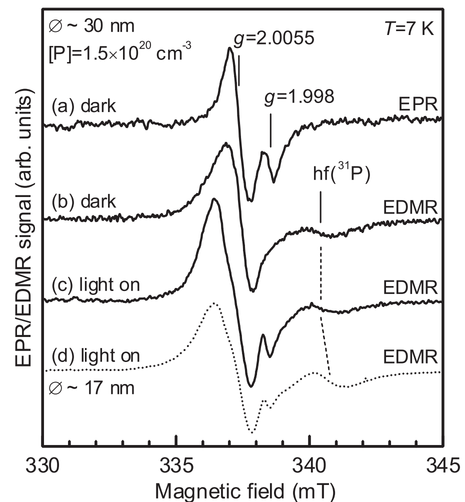

FIG. 4. (a) EPR, (b) EDMR, and (c) photoexcited EDMR spectra of a film of Si-NCs (∅ ~ 30 nm, [P] = 1.5×10^{20} cm^{-3}). (d) Photoexcited EDMR spectrum of a film of P-doped Si-NCs with 17 nm mean diameter ([P] = 6.5×10^{19} cm^{-3}).

nance is stronger, which highlights the importance of surface recombination in electronic transport through the Si-NCs network. No changes of the EPR spectrum are observed upon illumination of the film. DC-EDMR measurements reveal that the observed spin resonances lead to a quenching of the photocurrent ($\Delta I/I = -10^{-3}$), demonstrating that in this case, the paramagnetic states are centers for spin-dependent recombination of photogenerated electron and holes [24,25]. The absence of the $g = 1.998$ line in the dark EDMR spectrum suggests that the observation of this line in EPR and photoexcited EDMR is mainly due to electrons with a delocalized character, such as electrons in a metallic impurity band in a bulk semiconductor [26]. In contrast to isolated donor states [line hf(^{31}P)], such delocalized states are expected to contribute less to spin-dependent hopping conduction. Nevertheless, such electrons can recombine spin dependently, e.g., via Si-DBs, resulting in the observation of the $g = 1.998$ line in photoexcited EDMR [27]. The EDMR spectrum of a film of P-doped (6.5×10^{19} cm^{-3}) Si-NCs with mean diameter of 17 nm is also shown in Fig. 4 [curve (d)]. An upwards shift of the hf(^{31}P) line by 0.3 mT is observed with respect to the film of Si-NCs with 30 nm [curve (c)]. This corresponds to an enhancement of the magnitude of the hyperfine interaction, which results from quantum-confinement of the donor electron wave function in the Si-NCs [8]. It is interesting to note that such an effect already plays a role for Si-NCs with a mean diameter of 17 nm. The width of the hf(^{31}P) EDMR lines in Fig. 4 is about twice that of the hf(^{31}P) EPR lines in Fig. 4(b). This probably results from the fact that the two techniques are sensitive to different ensembles of P states for which inhomogeneous broadening is different. Inhomogeneous broadening can also be enhanced for samples with smaller mean particle diameter due to the effect of the Si-NCs surface and size distribution on the donor electron wave function [5].

In summary, we have achieved P doping of macroscopic amounts of freestanding Si-NCs grown from the gas phase, as demonstrated by observation of EPR resonances associated with substitutional P in the Si-NCs. The electrical conductivity of undoped and P-doped Si-NCs was studied using films composed of densely packed Si-NCs. A pronounced doping effect on the electrical conductivity of such films is observed. EDMR measurements demonstrate the direct participation of P donor and Si-DB states in the electronic transport through Si-NC networks: P donors and Si-DBs contribute to dark conductivity via spin-dependent hopping, whereas in photoconductivity, the same paramagnetic states are shown to act also as recombination centers. Distinct subsets of P donor (or defect) states are detected via EPR and EDMR, which demonstrates that the microscopic details of paramagnetic centers participating in electronic transport through the Si-NCs network are different from the ensemble average. We show that the selectivity of EDMR permits the investigation of fundamental problems in nanocrystals, such as the quantum confinement of the donor wave function. The high sensitivity of EDMR will also allow future investigations of much smaller ensembles of Si-NCs than accessible by EPR. Thus, EDMR measurements on ensembles of ~50 P donors in Si have been demonstrated recently [27].

We thank A. L. Efros and D. J. Norris for valuable discussions. Financial support from the EU (PSYNANO), DFG (Nos. SFB 631, GK 1240), Evonik Degussa S2B Nanotronics, and the state of North Rhine-Westfalia is acknowledged.

*pereira@wsi.tum.de

[1] D. J. Norris *et al.*, Nano Lett. **1**, 3 (2001).
[2] L. Levy, J. F. Hochepied, and M. P. Pileni, J. Phys. Chem. **100**, 18322 (1996).
[3] F. V. Mikulec *et al.*, J. Am. Chem. Soc. **122**, 2532 (2000).
[4] S. B. Orlinskii *et al.*, Phys. Rev. Lett. **92**, 047603 (2004).
[5] G. M. Dalpian and J. R. Chelikowsky, Phys. Rev. Lett. **96**, 226802 (2006).
[6] G. Cantele *et al.*, Phys. Rev. B **72**, 113303 (2005).
[7] S. C. Erwin *et al.*, Nature (London) **436**, 91 (2005).
[8] M. Fujii *et al.*, Phys. Rev. Lett. **89**, 206805 (2002).
[9] K. Sumida *et al.*, J. Appl. Phys. **101**, 033504 (2007).
[10] A. R. Stegner *et al.*, Nature Phys. **2**, 835 (2006).
[11] B. E. Kane, Nature (London) **393**, 133 (1998).
[12] R. Vrijen *et al.*, Phys. Rev. A **62**, 012306 (2000).
[13] J. Knipping *et al.*, J. Nanosci. Nanotech. **4**, 1039 (2004).
[14] S. Brunauer, P. Emmet, and E. Teller, J. Am. Chem. Soc. **60**, 309 (1938).
[15] J. Müller *et al.*, Phys. Rev. B **60**, 11666 (1999).
[16] A. Baumer, Ph.D. thesis, Technische Universität München, 2005, Germany.
[17] P. R. Cullis and J. R. Marko, Phys. Rev. B **11**, 4184 (1975).
[18] J. D. Quirt and J. R. Marko, Phys. Rev. B **7**, 3842 (1973).
[19] For a review, see P. M. Lenahan and J. F. Conley, Jr., J. Vac. Sci. Technol. B **16**, 2134 (1998).
[20] M. Gjukic, R. Lechner, and M. Stutzmann, German Patent Application No. 102005056446 2006.
[21] C. T. Kirk, Phys. Rev. B **38**, 1255 (1988).
[22] G. Lucovsky *et al.*, Phys. Rev. B **28**, 3225 (1983).
[23] W. Theiss, Surf. Sci. Rep. **29**, 91 (1997).
[24] M. Stutzmann, M. S. Brandt, and M. W. Bayerl, J. Non-Cryst. Solids **266–269**, 1 (2000).
[25] M. S. Brandt and M. Stutzmann, Phys. Rev. B **43**, 5184 (1991).
[26] N. Mott and W. Twose, Adv. Phys. **10**, 107 (1961).
[27] D. R. McCamey *et al.*, Appl. Phys. Lett. **89**, 182115 (2006).